The electroreflectance anisotropy of the interband edge in silver may be unique among metals. The onset must occur in an energy region where free-electron effects are small, and must have the proper symmetry to be affected by a longitudinal perturbation. In addition, final states must be available to which transitions can occur, with a small momentum transfer, at an energy lower than the direct edge. These criteria are met in silver.

In summary we have studied metallic electroreflectance on noble-metal single crystals with normally incident polarized light. By employing careful electrochemical techniques, reproducibly clean, unstrained surfaces were produced. We have discovered an anisotropic contribution to the signal on the (110) surface of silver which cannot be explained by previous charge-modulation or band-shifting theories alone but can be rationalized by a field-induced vectoral perturbation of the joint density of states.

†Prepared for the U. S. Energy Research and Development Administration under Contract No. W-7405-eng-82.

[1]J. Feinleib, Phys. Rev. Lett. 16, 1200 (1966).

[2]A. B. Buckman and N. M. Bashara, Phys. Rev. 174, 719 (1968).

[3]B. D. Cahan, J. Horkans, and E. Yeager, Symp. Faraday Soc. 4, 36 (1970).

[4]T. Takamura, K. Takamura, W. Nippe, and E. Yeager, J. Electrochem. Soc. 117, 626 (1970).

[5]R. M. Lazorenko-Manevich and T. N. Stoyanovskaya, Élektrokhimiya 8, 1113 (1972).

[6]R. Garrigos, R. Kofman, A. Jolivet, and J. Richard, Nuovo Cimento 8, 242 (1972); R. Garrigos, R. Kofman, and J. Richard, Nuovo Cimento 13, 272 (1973).

[7]W. J. Anderson and W. N. Hansen, J. Electroanal. Chem. 47, 292 (1973).

[8]J. D. E. McIntyre, in *Advances in Electrochemistry and Electrochemical Engineering*, edited by R. H. Muller (Wiley-Interscience, New York, 1973), Vol. 9, p. 61.

[9]F. Abelès, T. Lopez-Rios, and A. Tadjeddine, Solid State Commun. 16, 843 (1975).

[10]J. D. E. McIntyre, Surf. Sci. 37, 658 (1973).

[11]J. D. E. McIntyre and D. E. Aspnes, Bull. Am. Phys. Soc. 15, 366 (1970).

[12]J. R. Bower, Surf. Sci. 49, 253 (1975).

[13]D. Dickertmann, J. W. Schultze, and K. J. Velter, J. Electroanal. Chem. 55, 429 (1974).

[14]T. H. V. Setty, Indian J. Chem. 5, 5 (1967).

[15]A. G. Zelinski, R. Yu Bek, and A. I. Maslii, Élektrokhimiya 10, 1515 (1973).

[16]R. Rosei, C. H. Culp, and J. H. Weaver, Phys. Rev. B 10, 484 (1974); B. Segall and A. B. Chen, Bull. Am. Phys. Soc. 20, 334 (1975).

[17]C. E. Morris and D. W. Lynch, Phys. Rev. 182, 719 (1969).

[18]10 parts glacial acetic acid; 3 parts sulfuric acid; stainless steel cathode; 4 A/cm^2 with agitation, followed by the *in situ* hydrogen reduction treatment.

Stress-Induced Tricritical Phase Transition in Manganese Oxide

D. Bloch, D. Hermann-Ronzaud, and C. Vettier
Laboratoire de Magnétisme, Centre National de la Recherche Scientifique, 38042-Grenoble-Cédex, France

and

W. B. Yelon
Institut Laüe-Langevin, 38042-Grenoble-Cédex, France

and

R. Alben
Department of Engineering and Applied Science, Yale University, New Haven, Connecticut 06520

(Received 10 July 1975)

We have performed neutron scattering measurements of the antiferromagnetic order parameter in MnO as a function of temperature and applied uniaxial stress. We find evidence for a tricritical point for a stress at about 5 kbar.

Tricritical phase transitions have lately been the subject of many experimental and theoretical investigations.[1] In particular, the field-induced (metamagnetic) phase transitions in the iron halides, $FeCl_2$ and $FeBr_2$,[2] and in dysprosium aluminum garnet (DyAlG)[3] have provided examples of magnetic tricritical points. These three compounds are strongly anisotropic and their behav-

ior is usually discussed in terms of Ising-type models. The tricritical temperature T_{3c} separates the low-temperature region, where the antiferromagnetic-paramagnetic field-induced transition is discontinuous, from the high-temperature region, where this transition is continuous.

In this paper we present neutron-scattering results for a rather different type of magnetic tricritical phase transition, a transition induced by *stress* in the cubic Heisenberg NaCl-structure antiferromagnet MnO. This would then be the magnetic analog of NH_4Cl or ND_4Cl,[4] which present a discontinuous order-disorder transition at low pressure and a continuous one at high pressure.

Manganese oxide orders antiferromagnetically at about 118 K in the absence of applied stress.[5] The Mn^{2+} moments order in ferromagnetic (111) sheets which are stacked antiferromagnetically along a [111] direction. The four different [111] directions are associated with four types of "T domains," each with a spontaneous contraction along the corresponding [111] direction. The size of the contraction, characterized by the modification $\delta\alpha_0$ of the angle between the [100] and [010] axes is 1.12×10^{-2} rad at 4 K. In usual crystals the T domains are statistically equally distributed. The application of a [111] stress, however, favors the [111] T domain. A stress τ of several hundred bars is sufficient to suppress all other T domains and thus leads to a complete detwinning of the sample. The discontinuous character of the antiferromagnetic transition is much clearer in detwinned samples, for which it has been found[5,6] that with only a small detwinning stress, the order parameter σ drops abruptly to zero at the transition from about 60% of its $T=0$ K value. Suppression of the T domains in CoO under stress has been similarly observed using neutron-scattering techniques by van Laar, Schweitzer, and Lemaire.[7]

The application of a large [111] stress can lead to a continuous transition as may be seen from the following analysis. We consider a single T domain in the ordered state. A given Mn^{2+} has twelve nearest neighbors, six of which have spins parallel to its spin and six of which have antiparallel spins. The six next-nearest neighbors all have antiparallel spins. The interactions are represented by the Heisenberg Hamiltonian,

$$H=-2\sum_{\langle i,j\rangle}J_{ij}\vec{S}_i\cdot\vec{S}_j,$$

where the summation is on pairs of nearest-neighbor and next-nearest-neighbor spins $\vec{S}$. The principal effect of a distortion $\delta\alpha$ is to make the parallel and antiparallel nearest neighbors inequivalent. The exchange between parallel neighbors becomes $J_1^{+}=J_1^{0}-jJ_1^{0}\delta\alpha/2$ and that between antiparallel neighbors becomes $J_1^{-}=J_1^{0}+jJ_1^{0}\delta\alpha/2$. Here J_1^{0} is the exchange interaction in the absence of any distortion and j is a dimensionless number which gives the linear variation of exchange with distortion.

Within the molecular-field approximation the spin- and strain-dependent parts of the free energy can be written

$$\tilde{F}=6NS^2\sigma^2(J_2^{0}-jJ_1^{0}\delta\alpha)-NkT\left[\ln(2S+1)-\int_0^{\sigma}B_s^{-1}(\sigma')\,d\sigma'\right]+\tfrac{3}{2}V_m C_{44}(\delta\alpha)^2, \tag{1}$$

where N is Avogadro's number, J_2^{0} is the next-neighbor exchange, V_m is the molar volume, C_{44} is the cubic elastic constant, and B_s^{-1} is the inverse Brillouin function for spin S, where $S=\frac{5}{2}$ for Mn^{2+}. We develop $\tilde{F}$ as a power series in σ and minimize with respect to $\delta\alpha$ and σ. This gives, for the distortion,

$$\delta\alpha=12.5N\sigma^2jJ_1^{0}/C_{44}V_m+\tau/3C_{44}. \tag{2}$$

The order parameter σ is found from the equation

$$\sigma[2.1(T-T_2)+0.97(T-T_{3c})\sigma^2+0.71T\sigma^4]=\sigma \tag{3}$$

together with the condition that $\tilde{F}$ must be a minimum. The temperatures T_2 and T_{3c}, defined as

$$kT_2=-35J_2^{0}+11.7jJ_1^{0}\tau/C_{44},\qquad kT_{3c}=966(jJ_1^{0})^2/(C_{44}V_m), \tag{4}$$

are the all-important parameters determining the character of the transition.

When $T_2<T_{3c}$, the transition occurs at $T=T_1$, with

$$T_1=0.56T_2-0.13T_{3c}+(0.15T_{3c}^{2}-0.15T_{3c}T_2+0.32T_2^{2})^{1/2}. \tag{5}$$

The transition is then discontinuous, with the order-parameter discontinuity given by

$$\Delta\sigma = 1.01(T_{3c} - T_1)^{1/2} T_2^{-1/2}. \quad (6)$$

On the other hand, when $T_2 > T_{3c}$, the transition is continuous and occurs at T_2. The case when $T_2 = T_{3c}$ corresponds to the tricritical point.

The above mean-field analysis is, of course, only approximate. However, according to more sophisticated renormalization-group and series-expansion calculations, parameters analogous to T_2 and T_{3c} do describe the competition between discontinuous, continuous, and tricritical phase transition behavior. It is therefore useful to consider the values of T_2 and T_{3c} and their dependence on stress in MnO.

The transition in MnO at low stress is discontinuous with $T_1 = 118$ K and $\Delta\sigma = 0.6$. From (5) and (6), this gives $T_2 = 117$ K and $T_{3c} = 159$ K. As expected, $T_2 < T_{3c}$. In order to reach a tricritical point, T_2 must be driven up to T_{3c}. From (4) it is seen that T_2 depends explicitly on stress, while T_{3c} does not. Now the variation of T_2 with stress is essentially the same as the variation of T_1, and this has been measured for low stress to be 3 K/kbar. If T_{3c} is constant, we will obtain a tricritical point at 14 kbar. While variation in T_{3c} might in principle ruin the above argument, our experiments show that in fact a stress-induced tricritical point does occur in MnO. The tricritical stress is about 5 kbar rather than 14 kbar, a discrepancy which is understandable in light of the approximate nature of the theory.

We have performed elastic-neutron-scattering measurements of the order parameter in MnO as a function of temperature and applied [111] stress up to 6.6 kbar. The samples were single crystals of dimensions $2.9 \times 2.8 \times 1$ mm^3 with the [111] direction perpendicular to the largest face and the $[1\bar{1}0]$ and $[11\bar{2}]$ directions perpendicular to the other two faces. The sample was mounted with the $[1\bar{1}0]$ direction vertical in order to be able to study both the (111)- and $(11\bar{1})$-type reflections. The [111] stress was applied by means of pneumatically driven aluminium pistons. To improve uniformity, two lead foils 0.1 mm thick were inserted between the sample faces and the pistons. The stress was measured by two strain gauges fixed on the aluminum pistons and calibrated at room temperature and at 77 K, using a $5 \times 5 \times 5$-mm^3 beryllium copper sample of known elastic properties. The absolute error in the stress calibration is estimated to be less than 8% and, as described below, the stress uniformity over the MnO sample is estimated to be better than 6%. The assembly is mounted in a variable temperature cryostat which provides 0.1 K stability from 77 to 300 K. A germanium (533) monochromator was used to obtain an incident wavelength of 1.508 Å^{-1}. The experiments were performed on D1A, a high-resolution double-axis spectrometer at the Laüe-Langevin Institute in Grenoble. All measurements were ω scans restricted to the $(1\bar{1}0)$ plane.

The magnetic and lattice lines in MnO are completely separate. The effect of a relatively modest stress on a typical magnetic line (333) is shown in Fig. 1(a). The stress dramatically increases the intensity of this line due to detwinning of the sample. We have verified that the $(33\bar{3})$ reflection, which comes from a suppressed T domain, was absent. Another effect of detwinning, most clearly seen for nuclear lines [Fig. 1(b)], is the decrease of the width of the lines with initial stress. This is due to the supression of the $(22\bar{2})$-type reflection which has a different lattice spacing than the (222) reflection and thus broadens the observed line. A similar effect occurs when an unstressed sample is heated above the transition temperature [Fig. 1(c)]. We emphasize these effects since the presence of domains and the associated strains tend to "smear out" transitions and can make a discontinuous transition appear continuous. Indeed the presence of T-domain boundary-induced random strains has led in the past to confusion about the nature of the transition in MnO in zero applied stress. In Figs. 1(d) and 1(e) we show the effect of a large stress on the (333) magnetic line and on the (222) nuclear line. The lines move because of the stress-induced change in lattice spacing and they also broaden slightly because of inhomogeneous strain. The lattice spacing is a sensitive function of the applied stress, and the linewidth can give us a direct estimate of the strain homogeneity. Assuming that the mosaic spread, the resolution, and the strain distributions are Gaussian, we find that the full width at half-maximum of the strain distribution is 6% of the average applied-stress–induced strain. For a stress of 5 kbar, this corresponds to a smearing of the transition by less than 1 K.

In Fig. 2 we show results for the diffracted intensities as a function of temperature for several applied stresses. The order parameter σ is proportional to the square root of the diffracted intensity of any of the magnetic lines. We used the (333) line to determine σ since the stronger

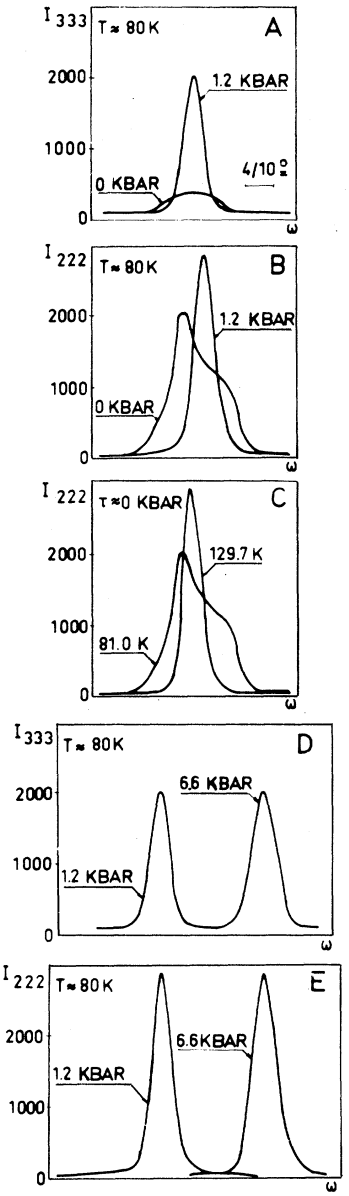

FIG. 1. (a) Effect of 1.2 kbar [111] stress on the (333) line. The $(\bar{3}\bar{3}\bar{3})$ line (not shown) is completely eliminated by this stress, indicating complete detwinning of the sample. (b) Effect of detwinning on the (222) nuclear line. (c) Comparison of the (222) line above and below the transition in the absence of applied stress. (d) The (333) line for stresses of 1.2 and 6.6 kbar below the transition ($T = 80$ K). (e) The (222) line for stresses of 1.2 and 6.6 kbar below the transition ($T = 80$ K).

(111) line is subject to serious extinction effects. We have normalized σ to 0.935 at 80 K.[6]

The antiferromagnetic transition is seen to be discontinuous[6] at 1.2 kbar, with $\Delta\sigma \sim 0.5$. At 1.9

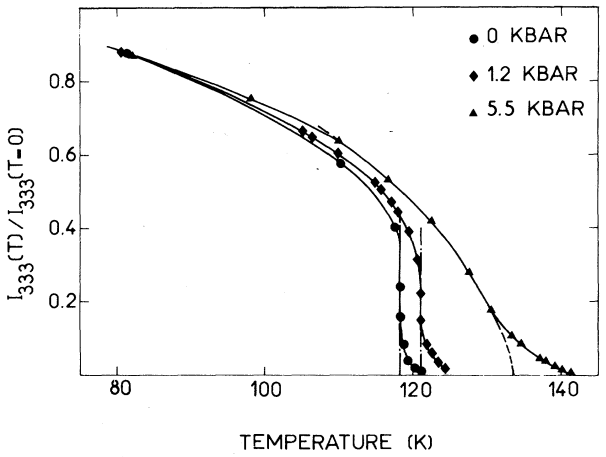

FIG. 2. Variation of the integrated intensity of the (333) line with temperature for several applied stresses.

and 2.4 kbar, the character of the transition is obscured by the strong increase in critical scattering above the transition. It was not possible to separate the Bragg and critical scattering contributions since we were working with relaxed collimation, and a consequently broad line, and the high background due to the stress apparatus was large compared to the critical scattering in the "wings." However, the discontinuity in σ is less than ~ 0.4. At high stress, the transition is apparently continuous, with the Bragg scattering going over into critical scattering, which then goes away over a temperature range of about 10 K. The persistence of scattering over this temperature range cannot be due to strain inhomogeneities for several reasons. More than 3-kbar inhomogeneity must be present to produce this effect, which seems physically improbable and would produce a linewidth for the (222) reflection much larger than that observed. In addition, the center of the magnetic reflection would be expected to shift with temperature since only the lattice spacings corresponding to the highest stress would be present at the highest temperature. Such an effect is not observed. Strong critical scattering above the transition has also been observed near the tricritical point in ND_4Cl and NH_4Cl.

In order to determine the continuous Néel temperature, we have tried to fit the experimentally observed behavior of σ with a law $\sigma = D[1 - T/T_N]^{\beta}$. For $\tau = 5.5$ kbar, this leads to $\beta = 0.30$ and $T_N = 133.5$. The value of β, although only approximate, might be compared with the value 0.25

expected for tricritical transitions, and the value 0.33 expected for a continuous transition in a three-dimensional XY-type model to which stressed MnO corresponds. The Néel temperature increases at the rate of ≈ 3 K/kbar, in agreement with previous results.[5]

We thank Dr. R. J. Birgeneau for helpful comments.

[1]See R. B. Griffiths, Phys. Rev. B 7, 545 (1973), for extensive references.

[2]I. S. Jacobs and P. E. Lawrence, Phys. Rev. 164, 866 (1967).

[3]N. Giordano and W. P. Wolf, Phys. Rev. Lett. 35, 799 (1975).

[4]C. W. Garland and B. B. Weiner, Phys. Rev. B 3, 1634 (1971); W. B. Yelon, B. Cox, P. J. Kortman, and W. B. Daniels, Phys. Rev. B 9, 4843 (1974).

[5]See D. Bloch and R. Maury, Phys. Rev. B 7, 4883 (1973).

[6]D. Bloch, R. Maury, C. Vettier, and W. B. Yelon, Phys. Lett. 49A, 354 (1974).

[7]B. van Laar, J. Schweitzer, and R. Lemaire, Phys. Rev. 141, 538 (1966).

COMMENTS

Comment on Signell and Holdeman's $I = 0$ np Phase-Shift Solutions at 330 MeV

Ronald Bryan*†
Research Institute for Theoretical Physics, University of Helsinki, SF-00170 Helsinki 17, Finland
(Received 2 June 1975)

I point out that one of the two solutions that Signell and Holdeman published for $I = 0$ np scattering at 330 MeV contradicts long-range one-pion-exchange dominance. This has interesting consequences, because recent theories of 2π exchange strongly favor this solution in the $^3D_1$ state.

In 1971 Signell and Holdeman pointed out[1] an ambiguity in phase-shift analyses of neutron-proton data at 330 MeV. They presented two solutions in their Letter, designated 1 and 2; these correspond almost identically to energy-independent solutions in papers IX[2] and X,[3] respectively, of the series of phase-shift analyses of nucleon-nucleon data published by MacGregor, Arndt, and Wright. Signell and Holdeman also showed graphs comparing the $\delta(^3S_1)$ and ϵ_1 phase parameters of solutions of type 1 and type 2 with several different N-N potential models including one-boson-exchange models, purely phenomenological models, and a model incorporating two-pion exchange; from their graph (Fig. 2 of the first citation in Ref. 1) it is evident that the models as a whole heavily favor the type-1 solution, at least insofar as the $\delta(^3S_1)$ and ϵ_1 phase parameters are concerned.

It is the purpose of this Comment, however, to point out that solution 1 has very little chance of being correct. This is because it predicts a $^3G_4$ phase shift which is in contradiction with one-pion-exchange (OPE) dominance at large distances.[4] This is illustrated in Fig. 1. There I show a graph of the OPE contribution to the $^3G_4$ phase shift over the 0–425-MeV range (with $g^2/4\pi = 14.9$ and $m_\pi = 137$ MeV/c^2), plus predictions for $\delta(^3G_4)$ by phenomenological potentials due to Lassila *et al.*[5] and Hamada and Johnston,[6] and by models incorporating two-pion-exchange contributions due to Lomon and Feshbach[7] and Lacombe *et al.*[8] The thing that all of these models have in common is the OPE potential, and that is why the $\delta(^3G_4)$ predictions all converge to the OPE prediction as the energy decreases.[9]

I also show in Fig. 1 $\delta(^3G_4)$ for the two solutions of Signell and Holdeman. One can see that the